

Current Characterisation for Ultra Low Power Wireless Body Area Networks

Fabio Di Franco, Christos Tachtatzis, Ben Graham, Marek Bykowski
David C. Tracey, Nick F. Timmons and Jim Morrison

WiSAR Lab
Letterkenny Institute of Technology
Port Road, Letterkenny, Co. Donegal, Ireland
{fabio, christos, ben, marek, david, nick, jim}@wisar.org

Abstract - The emerging area of body area networks (BAN) imposes challenging requirements on hardware and software to achieve the desired lifetimes for certain devices such as long term medical implants. In this paper, we propose a novel approach to the measurement and characterisation of the energy consumption of BAN devices. The approach uses a low cost energy auditing circuit and addresses the problem of accurately measuring low-level current consumption. This new technique will allow precise and analytical measurements of systems and components in terms of energy. This will help circuit designers minimise power consumption in BAN devices. Software engineers might use this approach to validate and optimise embedded code. Network engineers can optimise network parameters to reduce the power consumption of a single node. Adoption of the proposed technique will aid the development of ultra-low power wireless BANs. Results are presented on current characterisation for two wireless nodes.

Index Terms— Power Consumption, Current characterization, Energy efficiency, Embedded system design, Body Area Networks, Wireless Network software

1. INTRODUCTION

Technological breakthroughs in wireless body area networks will allow the development of affordable and efficient healthcare solutions for the escalating healthcare needs of a worldwide ageing population. Ultra-low-power wireless connectivity among devices placed in, on, and around the human body is seen as key to delivering this technology [1].

This has led to the concept of the Body Area Networks (BAN) with standardisation work currently under way by the IEEE 802.15.6 committee. BANs employ radio frequency technology for the communication between sensors and actuators. The traffic carried by these networks has diverse Quality of Service requirements such as bandwidths ranging from a few bits per minute up to 10 Mbps [2]. Additionally, extended device lifetime of up to ten years (i.e. for implantable devices) is also one of the strong challenges for the technology's success. The characterisation and optimisation of device energy usage to minimise power consumption is a key aspect of this research. Typical Body Area Network applications are summarised in Table 1 [3].

The following factors contribute to the energy efficiency of BAN devices:

1. Power efficient hardware. The component selection and board design are important for minimising current consumption.
2. Physical layer protocol efficiency. Physical layer aspects such as modulation schemes and encoding techniques can contribute to a power efficient architecture.
3. Data link layer design. The MAC must avoid and/or minimise idle listening, overhearing, over-emitting and other message overheads.
4. Software Implementation. The device drivers and software stack must be written to take advantage of features in the hardware and network protocols and designed to reduce power consumption, e.g. use dedicated hardware peripherals and put the microcontroller to sleep when possible.

Wearable BAN devices	Implanted BAN devices
EEG	Glucose sensor; Cardiac arrhythmia:
ECG	pacemaker, cardioverter, defibrillator
SpO2 pulse oximeter	Intracranial pressure sensing
Glucose	Wireless capsule drug delivery
Fall detection	Deep brain stimulation
Emergency call	retinal sensors, Parkinson's, epilepsy
Performance assessment	Insulin pump

Table 1 Typical BAN applications

The proposed current characterisation approach is based on the fact that it is difficult to assess the strength and weakness of BAN devices based on the datasheets. Simple analysis of the schematic and datasheets makes interaction difficult to predict if not impossible. For example, it is difficult to quantify the leakage current and the current drawn from pull up/down resistors from the mote schematics (when these are available) or to understand if a component draws current from general purpose lines (GPIO). Although these interactions when seen individually may draw small currents (in the order of 1-2 μA) they can cause a significant reduction in device lifetime over an extended period of time.

Another factor which is often not apparent from the study of the hardware specifications is transient behaviours which are not clearly defined in the datasheets and software implementation bottlenecks (i.e. scheduling delays). These can be significant and reduce the energy efficiency of the

overall system. Current estimation based only upon figures obtained from the datasheets can provide general indications but can not be relied upon for accurate device lifetime. The optimisation of the device drivers requires an in-depth knowledge of the specific device and requires validation of the functionality and power consumption of the device as the software is designed or modified.

The proposed energy auditing circuit in conjunction with an oscilloscope allows system designers to quantify the time spent and current consumption of any system states. This helps to build an understanding of the internal state of particular components and their interaction and to design and debug power efficient software. It also allows the designer to characterise the power performance of radio parameters, the physical and MAC layers.

A typical BAN sensor device will contain a microcontroller, a radio interface and a sensor. The typical operation can be summarised in the following steps:

1. Sleep
2. Wake and Sample Sensor(s)
3. Send reading or alert
4. Go to step 1

To highlight the importance of in-depth energy auditing consider a device with a low duty cycle that reports and samples infrequently. In this scenario the bulk of the energy consumption will be during the sleep state (step 1). For instance, a temperature sensor sampling once every 10 seconds and transmitting data to a base station has an average current draw of 13 μ Ah (see Section 3). If an additional 1 μ A is drawn due to any of the aforementioned inefficiencies the device lifetime will be reduced by 7.6%.

The rest of the paper is organised as follows. Section 2 describes the energy auditing circuit in detail, including its design, layout and validation. Section 3 presents the current consumption measurements during a typical sensing operation, the optimisation of radio and microcontroller drivers and the effect of using different modulation schemes.

2. ENERGY AUDITING HARDWARE ARCHITECTURE

The energy auditing hardware architecture allows us to profile the current drawn from the mote. It is a low cost architecture based on an amplifier board and an oscilloscope. A suitable multi-meter would give high accuracy, but does not give the required resolution in time to accurately profile the current drawn from the mote and to discern the different states and transitions, which is an important requirement as discussed earlier.

The amplifier board consists of a low-valued precision resistor placed in series to the current path that produces a small voltage drop, which is then amplified to serve as an output signal proportional to the current [4].

2.1. Hardware Design

Most current measurement applications employ either the low-side principle, in which the sense resistor connects in series with the ground path (between the ground of the mote and the negative power supply) or the high-side principle, in which it connects between the positive power supply and the mote power input. The low-side resistor adds undesirable

extraneous resistance in the ground path that cause the ground to bounce as the current in the system fluctuates, whereas the high-side sensing demands the sense amplifier to handle a high common-mode voltage. The energy auditing hardware architecture used here uses the high side current sensing principle to avoid ground related issues.

Using a simple sense resistor in series to the current path (between the power supply and the mote) would not give enough vertical resolution for the oscilloscope when the current consumption is under 1 mA. However, BAN devices in sleep state typically draw current below 1 mA and it is therefore a requirement to measure currents of the order of a few μ A. To resolve this issue an instrumentation amplifier can be used to amplify the voltage drop across the precision resistor. Then the amplified voltage drop can be connected to an oscilloscope.

The size of this precision sense resistor (R1) was chosen to be 4.99 Ω with 0.1% tolerance and power consumption of 250 mW. This resistor was chosen because of the low input voltage drop (which is equal to 100 mV when the mote draws 20 mA) and to guarantee enough sensitivity for accurately measuring low current consumption (typically 2 μ A).

The selected instrumentation amplifier chosen is an Analog Devices AD621. This is a monolithic instrumentation amplifier based on a modification of the classic three op-amp circuit. It has on-chip gain resistor for gains of 10 and 100. It guarantees a very small error gain ($\pm 0.05\%$), high linearity (maximum 10 ppm), and a Common Mode Rejection Ratio (CMRR) of 130 dB [5]. It guarantees a small total voltage offset that is completely cancelled by the calibration (see Section 2.3). The gain of the AD621 was set to 100 (short-circuit pins 1 and 8 as shown in Figure 1) and it generates a trans-conductance gain of 500 V/A. The AD621 has a maximum positive and negative supply voltage of ± 18 V.

In order to eliminate the need for an external power supply a micro-power DC/DC converter was incorporated to the design that powers up the instrumentation amplifier from a mini-USB connector. The DC/DC converter is a switching mode regulator which generates high frequency spikes. These could cause serious noise to the analogue components (such as the instrumentation amplifier) and were minimised by a careful choice of components and particular attention to the layout.

The micro power Linear LT1610 DC-DC converter was chosen because it works at a fixed switching frequency of 1.7 MHz making it easy to filter out this frequency using low Equivalent Series Resistor (ESR) decoupling capacitors. Moreover the LT1610 could be supplied from an input voltage between 1 to 8 V [6]. The positive and negative voltage supplies of the instrumentation amplifier are generated from the LT1610 as shown in Figure 2. The feedback resistor values (R11 and R12 as shown in Figure 2) were chosen to generate approximately ± 17 V to allow an output swing voltage between -15 V to 15 V and in this way allow a dynamic range up to 30 mA.

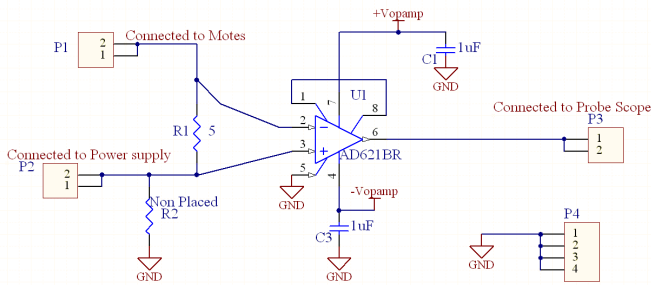


Figure 1. Amplifier circuit schematic

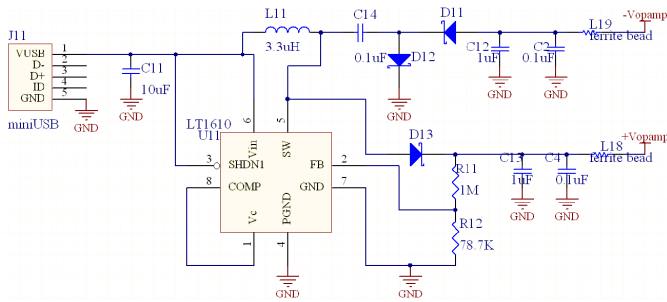


Figure 2. DC/DC regulator schematic

2.2. Board Layout

The board layout should be designed to minimise the current spikes generated by the DC-DC converter. These spikes return by the ground to the power supply. If the switching currents return to the supply through the same ground return as the analogue signal, the ground path of the analogue signal will be disturbed. In particular, the ground will bounce where the switching currents flow through the ground's resistance and inductance. The following design rules were used to avoid the current spikes propagated to the analogue ground:

1. The DC-DC switching currents must be localised to that circuit and must create an easy pathway (low impedance) for the switching current to return to the power input. It means that the power ground pin (pin4 of LT1610), the ground pad of the output capacitors (C2, C4, C12, C13) and the ground pad of the input capacitor (C1) must be physically located very close together and that a minimal impedance pathway must be created among them. Placing multiple vias between the ground pads and the power ground (on the bottom layer) reduces the inductance and resistance. The power ground was then connected to the main ground at the mini-USB port.
2. The feedback resistor (R12) ground pad was connected to the signal ground of LT1610 (pin7) and then to the ground star point. In this way, switching current will not circulate within the signal ground and will not affect the current regulation.
3. The star grounding point is the mini-USB supply. This is the reference point for all the other grounds on the board. The analogue ground is not affected by power ground because the circulation of the switching current

is localised to the power ground. In fact when the switch inside the LT1610 is closed, the switching current returns to the voltage input by LT1610 pin4 and when the switch is open, the switching current returns to the input capacitors by the output capacitors.

4. Short and wide lines were used to connect power components and reduce inductance and resistance. Schematic, layout and gerber of the low-cost energy auditing hardware are available in [7].

2.3. Calibration and Validation of the Test Setup

The validation of the test setup was carried out by placing the resistor R2 connecting P1 to an external power supply and connecting P3 to an oscilloscope that shows the voltage drop across the R1 resistor multiplied by a factor of 100.

Additionally, a multi-meter was connected in series between the power supply and P1 connector to validate these measurements. The Agilent 34405A multi-meter used which has accuracy of $\pm(0.05\%$ of the reading $+0.005\%$ of the full scale). A 1x probe scope was used with vertical resolution up to 2 mV/div. To minimise the quantisation error, the oscilloscope vertical scale must be set to the lowest level that keeps the signal within the dynamic range.

The system was calibrated by measuring the voltage offset at the output of the op-amp (P3 header) when the input of the op-amp is 0 V. This offset value is stored and subtracted from the measurements. This offset is composed of the offset due to amplifier board and due to the scope.

Without this calibration, the accuracy is poor for current values less than 50 μA . With calibration, the error becomes 1% for current consumption between 2 μA and 30 μA and less than 0.5% for current consumption between 30 μA and 30 mA.

3. EXPERIMENTAL RESULTS

This section presents the results of the current consumption during standard operations of a sensor mote; sleep, sense and transmit. Further to these, section 3.4 demonstrates how to use the proposed approach to optimise device drivers and section 3.5 shows how different modulation schemes affect power consumption. Our approach was applied to two wireless devices:

- Texas Instrument EZ430-RF2500 that includes the MSP430F2274 microcontroller and the CC2500 radio.
- A WiSAR designed mote which uses the MSP430F1611 microcontroller, the CC2420 radio and Sensirion SHT11 Temperature/Humidity Sensor [8]. It has key components in common with TelosB [9] but does not suffer from an additive 3 μA current consumption due to switches and buffers necessary to avoid current from flowing backward to USB circuitry.

3.1. Current Consumption of Different Power Modes of the Microcontroller

The current consumptions of the EZ430-RF2500 and WiSAR motes were measured when the microcontrollers were in active and in low power modes. In these tests, the radio voltage regulator and crystal oscillator were switched off and the sensor was in sleep mode. These tests were conducted at room temperature. Using IAR workbench, C code was

developed to put the microcontroller into active and low power modes. The measured current consumptions are shown in Table 2 and Table 3 for active mode and low power modes (LPMs) with master clock (MCLK) clocked at 1.1MHz.

eZ430-RF2500	Measured total current consumption of the mote
Microcontroller Active with MCLK=1.1MHz	480 μ A
LPM0	102 μ A
LPM3 with fACLK from internal VLO	1.3 μ A

Table 2. Current consumption in eZ430-RF2500

WiSAR mote	Measured total current consumption of the mote
Microcontroller Active with MCLK=1.1MHz	558 μ A
LPM0	61.3 μ A
LPM1	61.6 μ A
LPM2	13.6 μ A
LPM3 with fACLK from external xtal	2.7 μ A

Table 3. Current consumption in WiSAR mote

Measurements show that non-initialised ports resulted in an unnecessary extra current consumption of 50 μ A. For this reason all unused ports were set as outputs and driven low.

The mote was supplied from a 3 V power supply. The mote acts as a resistor and the current drawn changes proportionally according to the applied voltage. For example, increasing the supply voltage to 3.6 V on the EZ430-RF2500 causes current draw to increase by 20%.

The EZ430-RF2500 does not have an external crystal connected to the microcontroller and the mote can be put to LPM3 only using the internal inaccurate Very Low Oscillator (VLO) [10]. The VLO frequency drift is so high that will prevent the use of the EZ430-RF2500 in LPM3 state for periodic applications.

3.2. Current Consumption during Sensing

It is important to profile the mote during its actual sensing operation as part of its overall characterisation. Data is not processed or sent when measuring the sensing operation. The Sensirion SHT11 is a sensor chip used in the WiSAR mote that integrates temperature and humidity sensors with an ADC and 2-wire digital interface [8]. The measurement shows the total current drawn from WiSAR mote during a 12-bit humidity measurement. The different power states are shown in Figure 3:

- State 1: The microcontroller is in LPM0 and the SHT11 is sleeping. The total current consumption is 63 μ A (only 1.7 μ A due to SHT11)
- State 2: The microcontroller is active with MCLK 1.1 MHz sending a command strobe of (1 byte) to the SHT11 using the 2-wire digital interface.
- State 3: The microcontroller and the SHT11 are active: the SHT11 is performing the humidity measurement

and the microcontroller is monitoring the DATA line to establish when the measurement finishes. This state should last maximum 80 ms (doing a 12-bit measurement) according to the typical datasheet value [8]. However our measurements show that the SHT11 measurement is a two state operation not documented in the SHT11 datasheet: in 3a the SHT11 draws 220 μ A for 10.4 ms, in 3b the SHT11 draws 420 μ A for 60 ms.

- State 4: The microcontroller reads the 2-byte measurement from the sensor. The current consumption is equal to that of state 2.

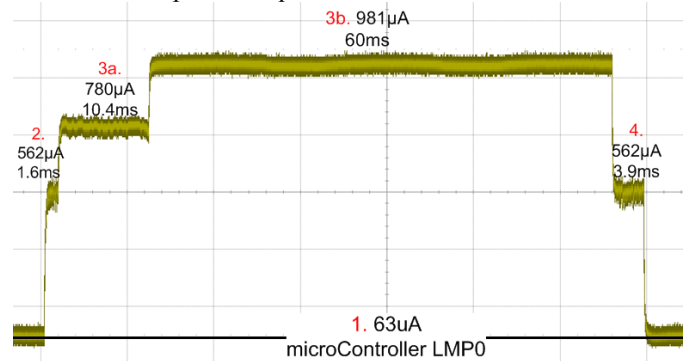


Figure 3. Current consumption profile of WiSAR mote during the Sensirion SHT11 operation

A temperature measurement with the SHT11 has the same current profile as a humidity measurement. If the temperature measurement is taken with 14-bit resolution, the state 3b lasts 230 ms.

3.3. Current Consumption Profile During Radio Transmission

This test focused on the different power states of the CC2500 radio on the EZ430-RF2500: from sleep mode to idle to calibration and finally to transmission. The tests use a custom build C library that allows full control of the CC2500 radio and MSP430.

Figure 4 shows the different power states of the EZ430-RF2500 supplied by 3 V when the CC2500 goes from sleep mode to transmission and the microcontroller is clocked at 1.1 MHz.

- State 1: The CC2500 radio is in sleep mode (digital voltage regulator and crystal oscillator off) and the microcontroller is in LPM0 clocked from the internal Digitally Controlled Oscillator (DCO) at 1.1 MHz.
- State 2: The microcontroller wakes up (a timer is initialised), the instructions for sending the radio to IDLE are processed and Chip Select (CS) is asserted (CS low)
- State 3: When CS goes low, the radio goes to IDLE starting the crystal oscillator and the voltage regulator. This causes a current spike to charge the capacitors. Subsequently, the microprocessor stays on and polls the Slave Output (SO) line until it goes high. When SO goes high, the crystal oscillator in the radio has become stable and SPI commands can be sent to the radio.
- State 4: The radio is in IDLE and the microprocessor goes from LPM0 to active every time it has to write a byte in

the TX FIFO. 50 bytes were sent from the microcontroller to the FIFO TX

- State 5: The radio is calibrating the frequency synthesiser and microcontroller in LPM0.
- State 6: The radio is transmitting at maximum power (1 dBm) with default factory settings (data rate is 115 kbaud). The payload data has 50 bytes and another 9 bytes of overhead are inserted automatically from the radio (preamble is 4 bytes, sync word is 2 bytes, length field is 1 byte and CRC is 2 bytes).
- State 7: When the 50 bytes have been transmitted, the radio automatically goes to IDLE. Then the microcontroller is notified with an interrupt which in turn wakes up and sends an instruction to send the radio to sleep.

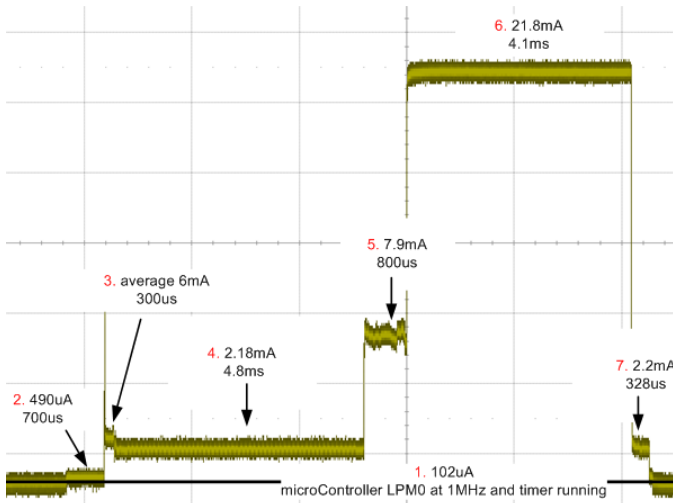


Figure 4. Current consumption profile of eZ430-RF2500 during a TX transmission

3.4. CC2500 and MSP430 Device Driver Library Optimisation

In this test the CC2500 and MSP430 libraries were optimised to reduce power consumption and duration of particular power states thus reducing energy cost. The power states of section 4 were optimised as below:

- State 1: The base current consumption is reduced to 1.3 μ A by keeping the microcontroller in LPM3 with the internal VLO.
- State 2: The microcontroller is clocked from the internal DCO set at 8 MHz. It increases the current consumption to 3.2 mA but reduces the time for processing at 100 μ s.
- State 3: By changing the default radio configuration (MCSM0.PO_TIMEOUT set to 0), the time for the radio to assert CS line is reduced to 150 μ s.
- State 4: By changing SPI clock frequency from 0.5 MHz to 4 MHz, the time to write 50 bytes in the TX FIFO is reduced from 4.8 ms to 0.65 ms.
- State 5: Performing the frequency synthesiser calibration only when necessary (MCSM0.FS_AUTOCAL set to 0 and

IOCFGx.GDOx_CFG to 0xA), the Phase Locked Loop (PLL) turn-on/hop time is reduced to 88 μ s.

- State 6: By changing the data rate from 115.2 kbaud to 500 kbaud and reducing the preamble from 4 bytes to 2 bytes, the time to transmit 50 payload bytes is reduced from 4.1 ms to 930 μ s.
- State 7: Having the microcontroller clocked at 8 MHz reduces the time to switch off the radio to 49 μ s.

The current profile after the optimisation is shown in Figure 5. The energy saving for each power state is shown in Table 4.

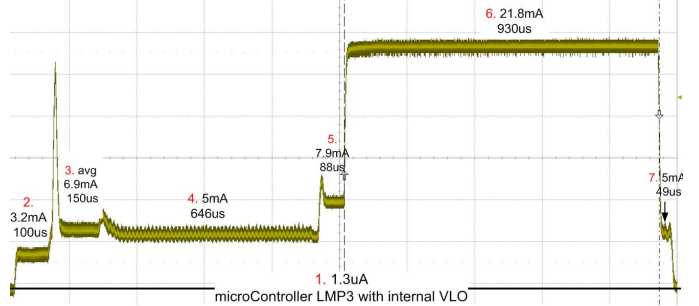


Figure 5. Current consumption profile after devices libraries optimization

Power state	Current drawn before optimization	Time before optimization	Current drawn after optimization	Time after optimization	Energy saved from optimization
1	102 μ A		1.3 μ A		98.7%
2	490 μ A	700 us	3.2mA	100us	6.7%
3	6mA	300 us	6.9mA	150us	42.5%
4	2.18mA	4800us	5mA	646us	68.0%
5	7.9mA	800us	7.9mA	88us	89.0%
6	21.8mA	4100us	21.8mA	930us	77.3%
7	2.2mA	328us	5mA	49us	66.0%

Table 4. Energy saved by device library optimization

Analysis of Table 4 shows that optimisation of the device drivers and libraries saves 76.3% overall compared to the implementation in Section 3.3 during a transmission of 50 bytes. The standby energy consumption is reduced by 98.7% when the microcontroller is kept in LPM3 instead of LPM1 (Section 3.3).

3.5. Impact of Modulation Schemes on Current Consumption

The CC2500 datasheet [11] reports the current consumption at different power levels but not the effect in current consumption using different modulations. The average current consumption measured during a transmission at 1 dBm was 21.8 mA for the Minimum Shift Keying (MSK) modulation and 14 mA for On-Off Keying (OOK) modulation as shown in Figure 6. This is due to the particular characteristic of the OOK modulation which means there is no transmission during a 0 bit. Other kinds of modulation such as Quadrature Amplitude Modulation (QAM) would also have affected the current consumption but unfortunately they are not supported by the CC2500 radio chip.

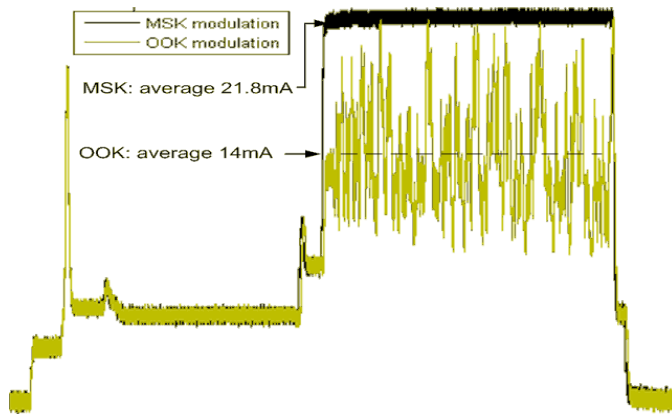


Figure 6. Current consumption comparison between MSK and OOK modulation

4. CONCLUSION

This paper presents a low-cost technique to measure current characterisation of ultra-low power BAN devices. The new energy auditing hardware developed by the WiSAR Lab guarantees an accuracy of less than 0.5% measuring current from 30 μ A to 30 mA and 1% for value from 2 μ A to 30 mA. The current consumption of two wireless motes was characterised.

Experiment 3.1 profiled current consumption of the microcontrollers in active mode and low power modes. In experiment 3.2 the monitoring of current consumption during a sensing operation exposed differences in performance when compared to data sheets; the recorded current profiles exposed states not documented in the data sheet. In Experiment 3.3 the energy auditing technique permits the identification of the different power states during radio transmission and in 3.4 the optimisation of the radio and microcontroller device libraries, resulting in a 76% energy saving compared to Experiment 3.3. Finally, experiment 3.5 illustrated the value of the technique in assessing the impact of different modulation schemes on current consumption.

The results show the value of in-depth energy auditing. The technique allows system level energy efficiency improvements, assists low-power hardware and software development and system validation. The WiSAR Lab will be using this technique to validate the design and implementation of new ultra low power MAC and routing layers and to measure their energy efficiency.

ACKNOWLEDGMENT

This work was carried out under the auspices of Enterprise Ireland Applied Research Enhancement (ARE).

5. REFERENCES

- [1] M. Patel, and J. Wang, "Applications, Challenges, And Prospective In Emerging Body Area Networking Technologies", IEEE Wireless communications, Feb 2010.
- [2] Daniel Lewis "802.15.6 Call for Applications – Summary" IEEE P802.15-08-0407-05
- [3] N. F. Timmons and W. G. Scanlon, "An adaptive energy efficient mac protocol for the medical body area network," International Conference on Wireless Communications, Vehicular Technology, Information Theory and Aerospace & Electronic Systems Technology (VITAE), May 2009.

- [4] X. Jiang, P. Dutta, D. Culler, and I. Stoica, "Micro power meter for energy monitoring of wireless sensor networks at scale," in Proc. 6th International Symposium on Information Processing in Sensor Networks IPSN 2007, 2007, pp. 186–195.
- [5] Analog Devices, "AD621 Datasheet," http://www.analog.com/static/imported-files/data_sheets/AD621.pdf, January 2001.
- [6] Linear Technology, "LT1610 Datasheet," <http://cds.linear.com/docs/Datasheet/1610f.pdf>.
- [7] WiSAR Lab "Research Outcome" <http://www.wisar.org/>
- [8] Sensirion, "SHT11 - Digital Humidity Sensor," http://www.sensirion.com/en/pdf/product_information/Datasheethumidity-sensor-SHT1x.pdf.
- [9] S. Polastre and Culler, "Telos: Enabling ultra-low power wireless research," in Proceedings of the 4th international symposium on Information processing in sensor networks, 2005.
- [10] Texas Instruments, "MSP430F22x2, MSP430F22x4 Mixed Signal Microcontroller (Rev. D)," <http://www.ti.com/lit/gpn/msp430f2274>.
- [11] Texas Instruments, "Low-Cost Low-Power 2.4 GHz RF Transceiver (Rev. C)," <http://focus.ti.com/lit/ds/symlink/cc2500.pdf>.